Pegylated, Steptavidin-Conjugated Quantum Dots Are Effective Detection Elements for Reverse-Phase Protein Microarrays

David Geho,[†] Nicholas Lahar,[†] Prem Gurnani,[‡] Michael Huebschman,[‡] Paul Herrmann,[†] Virginia Espina,[†] Alice Shi,[†] Julia Wulfkuhle,[§] Harold Garner,[‡] Emanuel Petricoin, III,[§] Lance A. Liotta,[†] and Kevin P. Rosenblatt*[,‡]

FDA-NCI Clinical Proteomics Program, Laboratory of Pathology, National Cancer Institute, National Institutes of Health, Bethesda, Maryland 20892, Office of Cellular and Gene Therapy, Center for Biologics Evaluation and Research, Food and Drug Administration, Bethesda, Maryland 20892, and Department of Pathology, Division of Translational Pathology, University of Texas Southwestern, Dallas, Texas 75390. Received December 2, 2004; Revised Manuscript Received March 24, 2005

Protein microarray technologies provide a means of investigating the proteomic content of clinical biopsy specimens in order to determine the relative activity of key nodes within cellular signaling pathways. A particular kind of protein microarray, the reverse-phase microarray, is being evaluated in clinical trials because of its potential to utilize limited amounts of cellular material obtained through biopsy. Using this approach, cellular lysates are arrayed in dilution curves on nitrocellulose substrates for subsequent probing with antibodies. To improve the sensitivity and utility of reverse-phase microarrays, we tested whether a new reporter technology as well as a new detection instrument could enhance microarray performance. We describe the use of an inorganic fluorescent nanoparticle conjugated to streptavidin, Qdot 655 Sav, in a reverse-phase protein microarray format for signal pathway profiling. Moreover, a pegylated form of this bioconjugate, Qdot 655 Sav, is found to have superior detection characteristics in assays performed on cellular protein extracts over the nonpegylated form of the bioconjugate. Hyperspectral imaging of the quantum dot microarray enabled unamplified detection of signaling proteins within defined cellular lysates, which indicates that this approach may be amenable to multiplexed, high-throughput reverse-phase protein microarrays in which numerous analytes are measured in parallel within a single spot.

INTRODUCTION

The pathophysiology of cancer is effected, in part, by proteins elaborated by diseased and normal cells within the tumor microenvironment (*1*). An important milestone in understanding tumorigenic processes is uncovering the nature of tumor cell signaling pathways (*2*). Certain classes of proteins form noncovalent associations, or networks, that comprise signaling pathways. With each association, one protein (a kinase) confers a posttranslational modification such as phosphorylation on its binding partner. This type of interaction is a fundamental means of cellular communication in a cellular environment and underlies the development of malignancy through potentiation of cellular motility, invasiveness, motility, proliferation, and evasion of apoptosis.

Reverse-phase protein microarrays (RPMAs; Figure 1) are an emerging high-throughput technology that offer a means to quantitatively measure both protein levels and posttranslational modifications of signaling proteins in clinical specimens (*3*−*6*). Current genomic techniques are unable to measure such modifications, which are important determinants of protein activity. In this assay, the lysates contain heterogeneous protein mixtures, or analytes, obtained from laser capture microdissected tumor cells extracted from individual patient specimens.

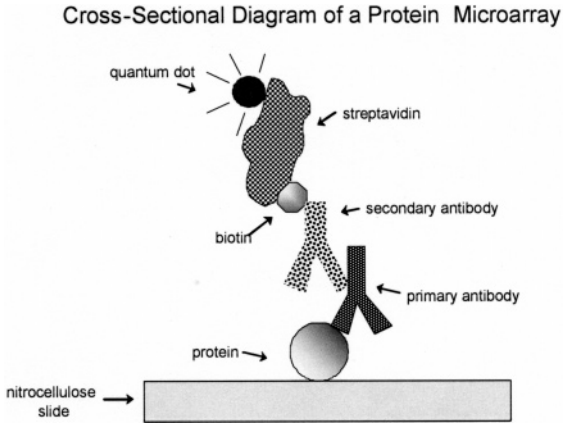

Figure 1. Reverse-phase microarray. In the RPMA, proteins extracted from cellular lysates are arrayed onto a nitrocellulose substrate and probed with a primary antibody. In turn, a biotinylated secondary antibody recognizes the presence of the primary antibody. The biotinyl groups are then detected by streptavidin linked to reporter molecules such as quantum dots or enzymes such as HRP that carry out catalyzed reporter deposition for signal amplification.

These lysates are noncovalently immobilized onto an array surface such as nitrocellulose and then probed by a variety of techniques. This reverse-phase format enables the measurement of low-abundance proteins from a minute amount of scarce clinical samples (on the order of nanoliters) and allows the clinical investigator or clinical lab specialist to compare numerous distinct patient samples, various clinical stages of cancer, mor-

[†] National Institutes of Health.
[‡] University of Texas Southwestern.
[§] Food and Drug Administration.
* Corresponding author. E-mail: kevin.rosenblatt@utsouthwestern.edu.

10.1021/bc0497113 CCC: $30.25
Published on Web 05/04/2005

phological subtypes, and uninvolved tissues in parallel for side-by-side comparisons of protein activity and signal pathway analysis.

The analytes are detected using an interacting molecule such as a recombinant protein, an antibody, small molecules such as drugs, DNA aptamers, or phage display libraries. Because the analytes can be analyzed in a denatured or native protein format, antibodies useful for western blotting to detect sequential epitopes can be utilized in addition to antibodies employed in ELISAs for conformational epitopes. In fact, RPMAs are especially useful in measuring phospho-specific events since these epitopes are usually masked and require denaturation of the target molecule prior to analysis. The presence of a bound primary antibody can then be visualized through the use of several technologies. For example, the presence of a bound biotinylated antibody can in turn be detected by streptavidin linked to a reporter molecule. This allows a single reporter system to be applied to various, different primary probes. Whereas DNA microarrays benefit from nucleic acid amplification for increased sensitivity, proteins cannot be similarly amplified. Therefore, the detection systems for protein arrays must have a built-in signal enhancement step. A variety of conventional labeling techniques, including radioactivity (*7*), chromagens, and fluorescence (*8*, *9*), have been used to report the presence of proteins on arrays. However, in their current forms, they often have significant limitations in terms of their sensitivity, dynamic range, durability, speed, safety, and ability for multiplexing.

When investigating clinical specimens, a reporter system with a broad dynamic range is required so that disparate quantities of input material can be effectively measured under a single format or experiment in which detection saturation is not easily achieved. A common means of expanding the dynamic range of a protein assay is through the use of fluorescent reporter molecules, and there is an abundance of commercially available organic fluorophores that have been used to tag biological molecules. Unfortunately, many organic fluorescent molecules lack the sensitivity of amplified chromogenic systems and are highly susceptible to photobleaching. Application of emerging nanotechnologies to biology and medicine has produced an alternative class of fluorescently labeled probes through the conjugation of inorganic fluorophores called quantum dots (QDs) to biological interacting molecules (*10*−*12*). QDs are fluorescent, semiconducting nanocrystals, ranging in size from 1 to 10 nm. These nanoparticle labeling agents possess broadband excitation bandwidths with narrow emission bandwidths, large extinction coefficients, and very high quantum yields that result in bright fluorescence. Because of these factors, QDs have distinct advantages over organic fluorescent reporter molecules. Moreover, due to their resistance to photobleaching, QDs produce signals that can be time averaged.

To evaluate methods that could increase the sensitivity and potential for multiplexing the reverse-phase microarray technology, we tested whether QDs could be used as reporter agents using this methodology. Further, we investigated the utility of hyperspectral image analysis in detecting primary, unamplified QD signals (*13*, *14*), which could dramatically improve the chances for high-throughput and rapid analysis. We report here the coupling of QD reporter molecules and hyperspectral imaging techniques that results in the detection of primary, unamplified signals in assays probing for the presence of signaling proteins present in cellular extracts. The detection of numerous unamplified signals within the same protein spot heralds the approach of truly multiplexed quantitative microarray assays for protein activity. This approach has potential utility in clinical settings, enabling selection of personalized therapeutic regimes (*15*).

MATERIAL AND METHODS

Cellular Lysate Preparation. Whole cell lysates were prepared in the following manner. Jurkat cells (clone E6-1, ATCC, Manassas, VA) were grown in RPMI 1640 media (Invitrogen, Carlsbad, CA) supplemented with 10% heat inactivated fetal bovine serum supplemented with 1 mM L-glutamine. Jurkat cells (3×10^6) were then treated with 0.5 μg/mL anti-Fas antibody (Upstate, Waltham, MA) per 1 mL of media at 37 °C in 5% CO_2 for 6 h in order to induce apoptosis. Treated Jurkat cells were harvested by centrifuging the cells at 4 °C for 10 min at 1000 rpm. Subsequently, the cells were washed twice in cold phosphate buffered saline (PBS). The cell pellets were then lysed in a buffer consisting of T-PER (Pierce, Rockford, IL), 2x Tris-glycine SDS loading buffer (Invitrogen, Carlsbad, CA), and β-mercaptoethanol (Sigma, St. Louis, MO). The cellular lysates were vortexed, centrifuged, and stored at −20 °C. A431 cell lysates generated from cells treated with EGF were purchased from a commercial source (BD Biosciences, Chicago, IL).

Reverse-Phase Microarrays. The reverse-phase microarrays were generated as previously described (*6*). Lysates, diluted 1:1 in sample buffer (1 mL of T-PER extraction buffer added to 950 μL of 2x SDS sample buffer and 50 μL of β-mercaptoethanol), were arrayed on nitrocellulose-coated FAST glass slides (Schleicher & Schuell Bioscience, Keene, NH) using a GMS 417 pin-and-ring arrayer (Affymetrix, Santa Clara, CA) that utilizes 500 μm^2 pins. The lysates were arrayed in serial dilutions with a negative control (sample buffer only) included. Approximately 1.5 nL per spot was arrayed, and the slides were stored at −20 °C in a desiccated environment (Dreirite, W. A. Hammond, Xenia, OH) or used immediately.

Immunostaining Procedure. Once the slides were arrayed, they were placed into 1X Re-Blot, mild solution (Chemicon, Temecula, CA), for 15 min to relax protein structure. After the Re-Blot was removed, the slides were washed two times for 5 min each in PBS. The slides were placed into I-Block dissolved in PBS/0.1% Tween-20 for at least 2 h (Applied Biosystems, Foster City, CA) and were then immunostained using an automatic slide stainer (Autostainer Dako Cytomation, Carpinteria, CA) using manufacturer-supplied reagents. Briefly, the slides were incubated for 5 min with hydrogen peroxide and then rinsed with high-salt Tris-buffered saline (CSA Buffer, Dako) supplemented with 0.1% Tween-20. The slides were blocked with avidin block solution for 10 min, rinsed with CSA buffer, and then incubated with biotin block solution for 10 min. After another CSA buffer rinse, a 5 min incubation with Protein Block solution was followed with air-drying. The slides were then incubated with either a specific primary antibody diluted in Dako Antibody Diluent or, as a control, only DAKO Antibody Diluent for 30 min. The primary polyclonal antibodies used in the study were specific for ERK and phosphoERK (Cell Signaling Technology, Inc., Beverly, MA) at dilutions of 1:2000 as demonstrated by western blots (data not shown). The slides were washed with CSA buffer. A secondary biotinylated goat anti-rabbit IgG H+L antibody (1:5000) (Vector Labs, Burlingame, CA) was incubated with the arrays for 15 min. For amplification

purposes, the slides were washed with CSA buffer and incubated with streptavidin−biotin complex for 15 min. After another wash with CSA buffer, the Amplification Reagent was added and incubated for 15 min.

For slides developed using the chromogen system, after washing with CSA buffer, streptavidin−horseradish peroxidase (HRP) was added for 15 min, followed by a CSA buffer rinse; slides were incubated in diaminobenzidine (DAB) chromogen diluted in Dako DAB diluent for 5 min. After the chromogen incubation, the slides were washed in deionized water and imaged using a text scanner. For slides developed using QDs and catalyzed reporter amplification instead of streptavidin HRP, pegylated-Qdot 655-PEG-Sav or nonpegylated-Qdot 655-Sav diluted in QD Buffer was incubated for 15 min on the slides (QD reagents obtained from Quantum Dot Corporation, Hayward, CA). The slides probed with QDs were visualized using 254 nm epifluorescent UV lamps in a FluorChem cabinet system (Alpha Innotech, San Leandro, CA). The emission signal was visualized using a 655 nm narrow bandwidth emission filter (Omega Optical, Brattleboro, VT). Signal intensities for both the chromogen and fluorescent systems were measured and quantified using ImageQuant (version 5.2) (Molecular Dynamics) data analysis software.

A noncommercial hyperspectral imaging microscope was used for detecting proteins labeled without the use of catalyzed reporter amplification (*13*). Arrayed slides were pretreated with 1X Re-Blot and I-Block as described above followed by avidin and biotin blocking and then incubation with the DAKO Protein Block solution. After a 30 min incubation with the primary antibodies and subsequent incubation with the biotinylated secondary antibody, the slides were then exposed directly to the pegylated-Qdot 655-PEG-Sav reagent for 15 min. After being washed, the slides were dried and analyzed on the hyperspectral imaging system using a spectrophotometer coupled to a CCD camera. The slit width was 50 μm, and a 100 W Hg lamp was used for excitation. Continuous spectra between 549 and 666 nm were collected for each array.

Calibration of Hyperspectral Imaging System. During the imaging of the unamplified slides on the hyperspectral imaging system, slightly shorter wavelengths were observed from those reported by the manufacturer. To determine whether those values were a result of our imaging system or image analysis package, we calibrated our system using two monochromatic light sources. Briefly, the hyperspectral imaging microscope was configured with the *f*/6.5, $^1/_2$ meter spectrometer and cooled CCD camera. (For the original slide measurements, it was configured with a *f*/1.2 holographic spectrometer, photointensifier, and cooled CCD camera.) The measurement was made by first illuminating an unamplified specimen slide and recording the fluorescence emitted by the QDs used in the labeling reactions. The excitation illumination was provided via an Olympus U-MWIB filter cube (excitation 460−490 nm and emission LP 515 nm). Next, red (632.8 nm) and green (532 nm) lasers were directed through the microscope objective lens and similarly recorded on the same CCD camera array. The QD and laser spectra are overlayed pixel by pixel (Figure 5A). The wavelength scale calibration is provided by the known laser wavelengths. The wavelength measurement of the QD peak was determined from a simple Gaussian fit of the peak. The instrument function of the spectrometer was not subtracted from the spectra before a fit was made, but a spectral image of a non-QD region was subtracted from the data image before fitting the spectra. Ten peaks were measured from different areas of the image cube acquisition. An error of ~1 nm from the measurements and an estimated QD product uncertainty of ~1 nm give a combined error of ~1.414 nm.

RESULTS

Streptavidin-conjugated quantum dots were incorporated into a standard reverse-phase microarray assay to determine their utility as reporter molecules for this type of high-throughput proteomic test (*3*, *6*, *16*). Qdot 655 streptavidin conjugates were used to detect the presence of bound primary antibody/biotinylated secondary antibody complexes on protein lysates arrayed on nitrocellulose surfaces using an Affymatrix robotic arrayer. As a test system, a Jurkat T-cell population was treated with anti-FAS antibody, which induces apoptosis (*17*). This population of induced cells expresses detectable levels of activated ERK signaling protein based on previous laboratory experience and provided an excellent testing system for phosphoactivation of signaling proteins (data not shown).

Scanning/Detection Modalities. After blocking unbound nitrocellulose sites, arrays bearing immobilized cellular lysates were incubated with a rabbit anti-human ERK antibody. Following the washing steps, a biotinylated goat anti-rabbit secondary antibody was incubated for detection of bound anti-ERK primary antibody. To serve as background controls, identical slides were incubated without primary antibody (antibody diluent only). A secondary biotinylated anti-rabbit antibody was then incubated with the arrays. After washing, signal enhancement utilizing catalyzed signal amplification (CSA) was performed. Signal amplification via catalyzed biotinyl tyramide deposition is an effective tool for enhancing the sensitivity of immunoassays and has been previously shown to be useful in detecting intracellular signaling proteins using reverse-phase microarrays (*18*). Subsequently, the arrays were incubated with the Qdot 655 streptavidin reagent. The QD-probed array was scanned using an Alpha Innotech FluorChem imager using an excitation wavelength of 254 nm and emission measured at 655 nm (Figure 2A,C). Several scanning modalities were employed (data not shown), with the most effective signal-to-noise achieved using an Omega Optical filter made for assessment of 655 nm fluorescent emissions (20 nm bandwidth centered at 655 nm with added heavy blocking of wavelengths in the IR and UV ranges).

Nonspecific QD Interactions. While strong signals were observed within the protein spots after incubation with the primary, secondary, and streptavidin reagents, a similar signal was also present on spots incubated only with secondary reagent and the Qdot 655 streptavidin conjugate (Figure 2A). A similar level of background staining was not found in assays performed with the same secondary antibody reagent and a streptavidin-horseradish peroxidase conjugate followed by chromagen deposition with DAB (data not shown). The Qdot 655 streptavidin conjugate signal was restricted to the protein spots and was not present on the blocked nitrocellulose surface, indicating that molecular constituents of the cellular protein extracts were strongly binding to the QD conjugates in a dose-dependent manner.

Reduction of Nonspecific Binding Using Pegylated QD Conjugate. To decrease nonspecific binding, a modified form of streptavidin-conjugated QDs, Qdot 655-PEG-Sav, was used as the detection molecule in the

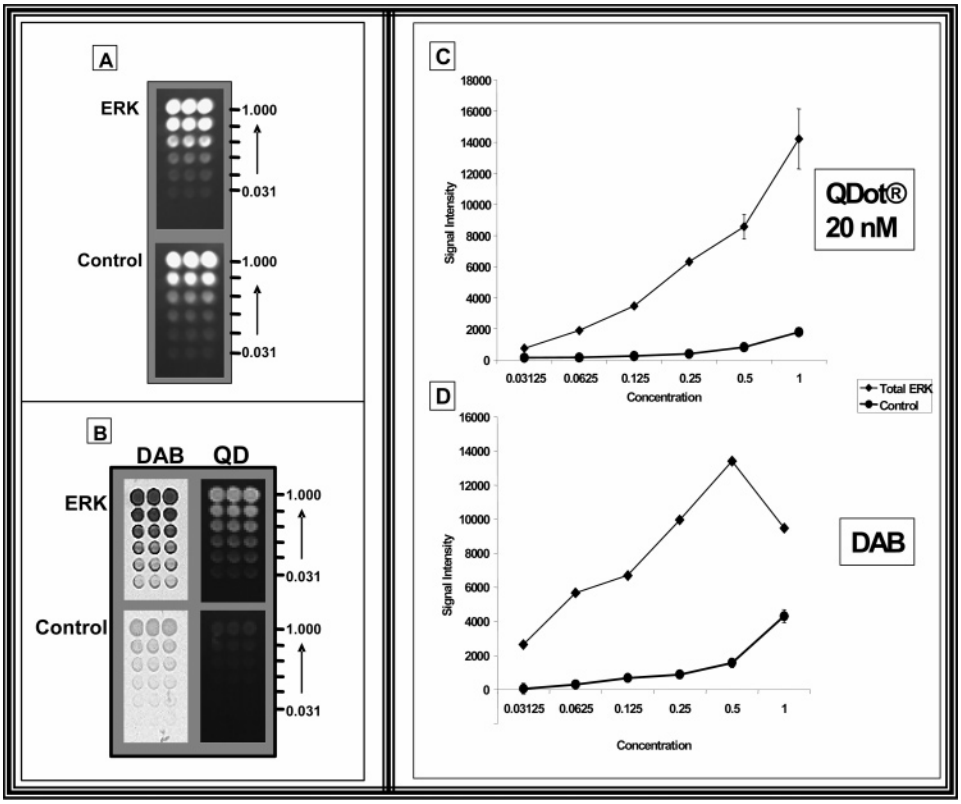

Figure 2. Protein extract binding properties of Qdot-655-SAV conjugates. Jurkat cell lysates, from cells treated with anti-FAS antibody, were arrayed upon nitrocellulose slides in serial dilutions. The array surfaces were then probed with anti-Erk antibody and subjected to biotinyl tyramide amplification. (A) Qdot-655-SAV conjugate (10 nM) was incubated on the arrays. The Qdot-655-SAV conjugate bound equally well to protein spots incubated with anti-ERK antibody or with buffer alone. (B−D) Then, either streptavidin-HRP (B, D) or Qdot 655-PEG-Sav (B, C) (20 nM) were incubated on the arrays. The signal produced by the amplified QDs resulted in a signal intensity per protein spot comparable to that of the standard colorimetric signal (DAB). Low background binding by the pegylated QD was observed. For visualization, the slides probed with QDs were excited using 254 nm UV light for 2 min and visualized using a 655 nm narrow-bandwidth (20 nm) emission filter.

RPMA format. This modification involved the introduction of poly(ethylene glycol) groups onto the streptavidin−quantum dot conjugates. In contrast to the nonpegylated form of the streptavidin-quantum dot conjugate, Qdot 655-PEG-Sav markedly improved the assay by decreasing the intrinsic binding characteristics of the streptavidin QDs to the protein spots (Figure 2B). Only in the presence of a bound primary antibody did Qdot 655-PEG-Sav bind strongly to the protein spots, indicating that the QD signals were limited to the presence of exogenously added biotinylated secondary antibody. Moreover, an identical array was concomitantly analyzed using the chromogen-based assay with DAB deposition as the reporter mechanism, and this also showed a similar staining pattern. The chromogen-based assay was scanned for quantitation using a standard 12-bit text scanner (Figure 2B), while the Qdot-probed array was scanned using an Alpha Innotech FluorChem imager using an excitation wavelength of 254 nm and emission measured at 655 nm (Figure 2C). The QD assay produced an antigen-dependent signal that was linear with a wide dynamic range. Detectable signal was present within the same analyte concentration range observed with the DAB-based chromogenic system; however, the text imaging system was unable to effectively measure the relative amount of chromagen that was deposited at higher protein concentrations due to saturation of the chromagen signal. The QD reporting system, on the other hand, performed well at higher signal intensities, and the dynamic range was significantly broader than the colorimetric method.

Generation of Time-Averaged Signals. One limitation of chromogen-based microarray assays is that only one time period for the development of signal through chromagen deposition can be chosen, and it must be committed to prior to assay performance. This can be a complicating factor in complex assays wherein multiple cellular lysates are arrayed on the same substrate with varying amounts of target proteins present in different dilution curves. The stability of QDs, in addition to their resistance to photobleaching, allows them to be imaged multiple times, for extended periods of time, to capture the linear portions of markedly different dilution curves located on the same array surface. To demonstrate the time-dependence of the quantum dot signal, Jurkat cell lysates, from cells treated with anti-FAS antibody (Figure 3A,B), were arrayed in serial dilutions. The array surfaces were then probed with the anti-ERK antibody. An amplification step followed with deposition of biotinyl tyramide. Qdot 655-PEG-Sav (10 nM) was then incubated on the arrays. The same slide was exposed to UV excitation (254 nm) at 30, 45, and 60 s time intervals. Increasing excitation times increased the signal emission by the QDs, while the background produced by the controls did not increase significantly. This experiment demonstrates the versatility of QDs in generating time-averaged signals. The titration of exposure times allowed the linear portions of various dilution curves to be elucidated in the same assay. Such control over the exposure time cannot be achieved with chromogenic assays, where only one development time is possible.

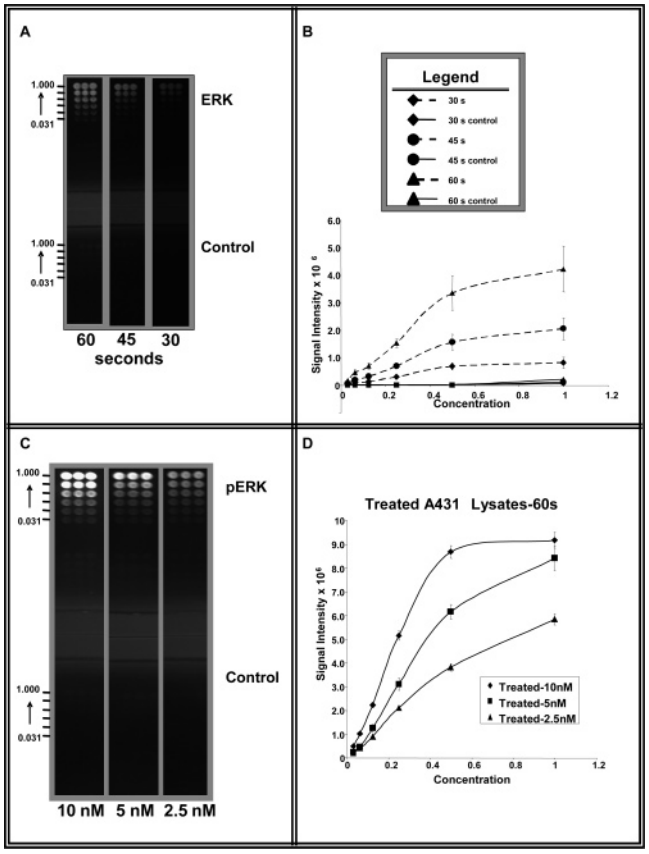

Figure 3. Concentration and time dependence of quantum dot reporter reagents. (A, B) Jurkat cell lysates, from cells treated with anti-FAS antibody, were arrayed upon nitrocellulose slides using serial 1:1 dilutions, probed with an anti-ERK antibody, and subjected to biotinyl tyramide amplification. For background controls, identical slides were incubated without antibody (antibody diluent only). Following the antibody probes, either streptavidin−HRP or Qdot 655-PEG-Sav (10 nM) were then incubated on the arrays. Flourescent slides were exposed to UV excitation (254 nm) at 30, 45, and 60 s time intervals. Increasing excitation times increased the signal emission by the QDs, while the background produced by the controls did not increase significantly. (C, D) EGF-treated A431 lysates were arrayed upon nitrocellulose slides in 1:1 serial dilutions and probed with anti-phosphorylated ERK antibody. For background controls, identical slides were incubated without antibody (antibody diluent only). Following the antibody probes, the slides were then incubated with either streptavidin−HRP or Qdot 655-PEG-SAv. The QD reagent was used at concentrations of 10, 5, and 2.5 nM. A clear dose dependence, based on the amount of QD conjugate added to the system, was observed.

Application of QDs to Alternative Cellular Lysates. To demonstrate the broader applicability of QD detection reagents in reverse-phase arrays, an alternative cellular lysate population was chosen. An epidermal growth factor-treated A431 epidermoid tumor cell line was arrayed on nitrocellulose slides in serial dilutions. The immobilized lysates were then probed with a rabbit anti-human polyclonal antibody that detects phosphorylated ERK (pERK), an activated form of the ERK signaling protein. A secondary biotinylated anti-rabbit antibody was then incubated with the arrays. Again, for the background control, no primary antibody was incubated on the array prior to the addition of a biotinylated anti-rabbit secondary antibody. After an amplification step using the biotinylated tyramide system, the slides were then incubated with Qdot 655-PEG-SAv at varying concentrations (10, 5, and 2.5 nM). The QD-treated slides were then subjected to 254 nm UV excitation, and a 655 nm narrow bandwidth filter was used during imaging (Figure 3C,D). While treated A431 cells did not reveal large increases in total ERK protein levels compared to untreated controls, a large increase in pERK levels was detected after exposure of the cells to EGF (data not shown). EGF is known to lead to phosphorylation of ERK protein (19); this demonstrates the utility of the assay for measuring posttranslational modifications and, thus, protein activation, which is not possible with genomic assays such as DNA microarrays. This experiment also demonstrated that the Qdot 655-PEG-SAv reagent could be applied to an alternative cellular lysate. Furthermore, the dose dependence of the QD signal was demonstrated by greater signal production, with increasing concentration, for a given protein.

Hyperspectral Imaging of QD Microarrays. With present imaging modalities, QD signals are undetectable when used in an unamplified system in RPMAs (data not shown). Hyperspectral imaging enables high-sensitivity scanning for the presence of multiple fluorophores (*13*, *14*). To this end, we tested whether the hyperspectral imager could detect significant signals from unamplified QD RPMA (Figure 4A−D). Indeed, a clear, significant QD signal above background was detected on an unamplfied microarray surface. Further, this measurement was performed on a microarray experiment that had been performed over six months previously, demonstrating the long life of these reporter molecules. Of note, the imaging analysis from our wavelength-calibrated system revealed that the peak emission spectrum was located at 648 nm, rather than the 655 nm emission specified by the supplier, indicating a slight blue-shift in the emission spectrum in our assays (Figure 4E).

Because of the stability of QD emissions over time, several different measurements of the microarrays can be taken at different times to enable optimization of the measurements or for verification of the measurements by different researchers. The hyperspectral image shown below (Figure 4), which had better S/N than at other dates of scanning, revealed a lower-than-expected emission maximum for the QDs (Figure 4E). This experiment indicated that the peak fluorescence of the 655-PEG-SAv reagent, when scanned at that date, was approximately 648 nm. The calculated combined error in our system due to an error of measurement of ~1 nm and an estimated QD product uncertainty of ~1 nm was ~1.414 nm, suggesting a true decrease in the emission wavelength from that reported by the company. To determine whether those measured values resulted from errors in the detection system, a two-laser calibration was performed (Figure 5A). Interestingly, a time-dependent decrease in peak maximum is apparent from the different measurements (Figure 5B).

DISCUSSION

One fundamental goal of clinical proteomics is the development of high-throughput tools that enable limited amounts of patient tissue specimens to be probed for the presence of molecular derangements. RPMAs represent one type of several high-throughput proteomic platforms currently being developed for use in clinical trials. This array format has shown great promise for phosphoproteomic profiling by effectively measuring cellular signaling events. Given the limited amount of material available in biopsy tissue specimens, there is an ongoing effort to improve the sensitivity, robustness, and versatility of RPMAs, so that the maximum amount of information can be extracted from patient specimens. The development of more sensitive detection technologies for

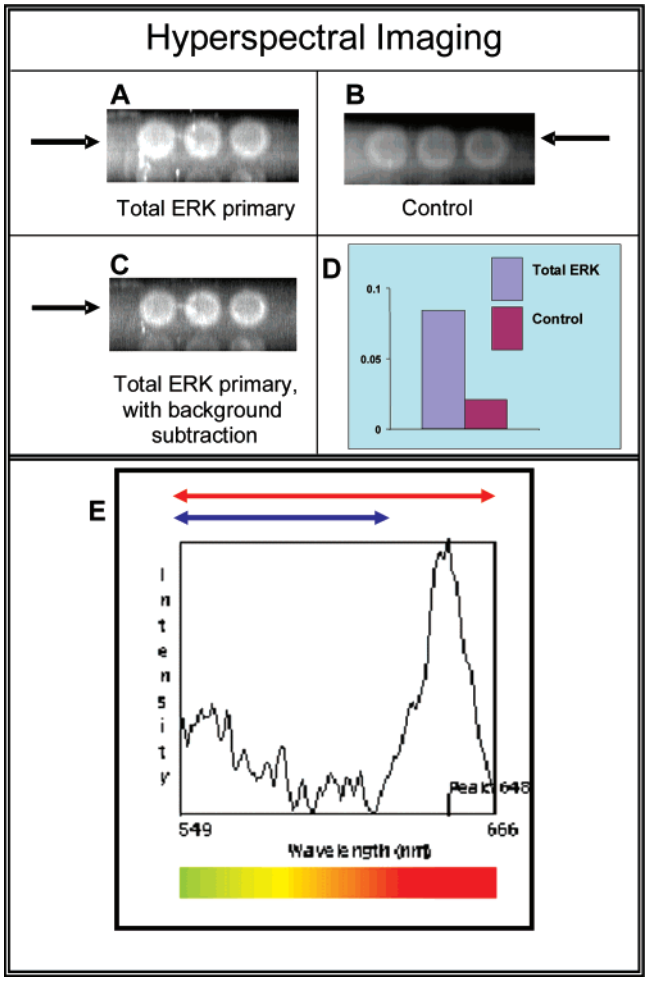

Figure 4. Hyperspectral imager detection of unamplified QD signal. Jurkat cell lysates, from cells treated with anti-FAS antibody, were arrayed upon nitrocellulose slides in a serial dilution. The array surfaces were then probed with anti-ERK antibody. As a background control, an identical slide was incubated without antibody (buffer only). A secondary biotinylated goat anti-rabbit antibody was then incubated with the arrays. Then, Qdot 655-PEG-Sav (20 nM) was incubated with the arrays. The signal produced by the unamplified QDs resulted in a signal detectable by hyperspectral imaging (A, C). Low background binding by the pegylated QD was observed (B). Relative fluorescence intensity is plotted in (D) to compare the signal from the array probed with the primary antibody (A) and the array without the primary antibody (B). The background, non-QD-dependent fluorescence (blue arrow in Figure 4E) was subtracted from the entire continuous spectrum (red arrow in Figure 4E) collected between 549 and 666 nm, resulting in an image signal mostly comprised of QD 655 nm-dependent light. Note, the peak emission spectrum was at 648 nm, an apparent blue-shift from the reported 655 nm peak from the commercial source (E).

protein arrays is being aided by recent developments in nanotechnology.

QDs are a recent example of an emerging nanotechnology. These nanoparticle-scale semiconductor crystals have wide excitation properties and narrow bandwidth emissions, which are generated primarily from elements in Groups II−VI or III−V of the periodic table (*20*, *21*). The emission wavelength can be tuned from the blue to the near-infrared by varying the size and chemical composition of QDs. Also for the same composition of QDs, the smaller the QD, the shorter its emitted wavelength. QDs have higher molar extinction coefficients when excited in the lower wavelength region of the spectrum. For example, QD 605 streptavidin conjugates (by Quantum Dots Corporation, Hayward, CA) have extinction coefficients ranging from 650 000 M^{-1} cm^{-1} at 600 nm to 3 500 000 M^{-1} cm^{-1} at 400 nm and even higher coefficients when excited with higher energy photons. In contrast, fluorescein has a maximum extinction coefficient of 80 000 M^{-1} cm^{-1} (*22*).

Coupled with their dimensional similarity to biomacromolecules, QD conjugates have been shown to be well suited as potential agents for molecular profiling and imaging (*10*, *11*, *20*−*22*). The quantum yields of most organic dye molecules are often decreased upon conjugation to biomolecules. However, higher quantum yields of QD conjugates (up to 80%) that remain unaffected by conjugation to biomolecules have been reported (*22*). Of note, QDs have been used in the development of a filtration-based protein microarray technique that can overcome the diffusion limit and enhance the overall performance of protein microarrays (*23*). The arrays used in that study consisted of an immobilized protein that bound a labeled analyte. Such an array, a forward-phase array, is not optimal for the analysis of heterogeneous clinical specimens and can suffer from lack of unmatched antibody affinities on a single array. The RPMA, as used in our present study, may be a more clinically applicable assay system in that the proteins from cellular lysates are arrayed directly onto a substrate, and since each analyte is measured one at a time, a direct comparison between patients, cell types, or therapeutic response can be evaluated. Direct immobilization of limited target proteins is required in order to realize protein microarrays in a clinical setting. This heterogeneous protein mixture requires a much more sensitive assay than is required for the capture (or forward-phase array) format.

One of the challenges in using QDs for biological studies is the design of hydrophilic QDs that can adapt to various biological environments. Surface coatings such as poly(ethylene glycol) and peptides have been used to decrease nonspecific binding, in the case of PEG, and to provide targeting motifs, in the case of peptides (*24*). QDs coated using an amphiphilic poly(acrylic acid) polymer or PEG are stable in vivo yet have different circulating half-lives (*25*). In the present study, pegylation of streptavidin-conjugated QDs improved the specificity of the binding interactions. Nonpegylated conjugates demonstrated high background binding to protein spots, which was not found with the pegylated conjugate.

QDs have symmetrical, narrow emission peaks unlike organic dyes, which possess asymmetrical and wider emission peaks, especially in the red region of the spectrum. Moreover, the large Stokes shifts between the excitation and emission spectra result in little autofluorescence when using a single common excitation wavelength in the high-UV range for all the different QD colors used in the same assay. These properties lead to minimal overlap, reducing spectral cross-talk between adjacent colors and enabling the possibility of simultaneous analysis of multicolor QDs with multiple narrow bandwidth filters. However, hyperspectral imaging tolerates overlapping spectral signatures. The characteristic property of simultaneous excitation of multicolor QDs with a single light source without appreciable energy transfer among different molecules makes them attractive for numerous biological applications. As it is possible to produce QDs with various emission wavelengths, one potential use of this reporter system is for highly parallel multiplex probing of numerous proteins on a single array. An important step forward toward this goal is the integration of hyperspectral imaging, which enables the detection of mutltiple unamplified QD wavelengths in

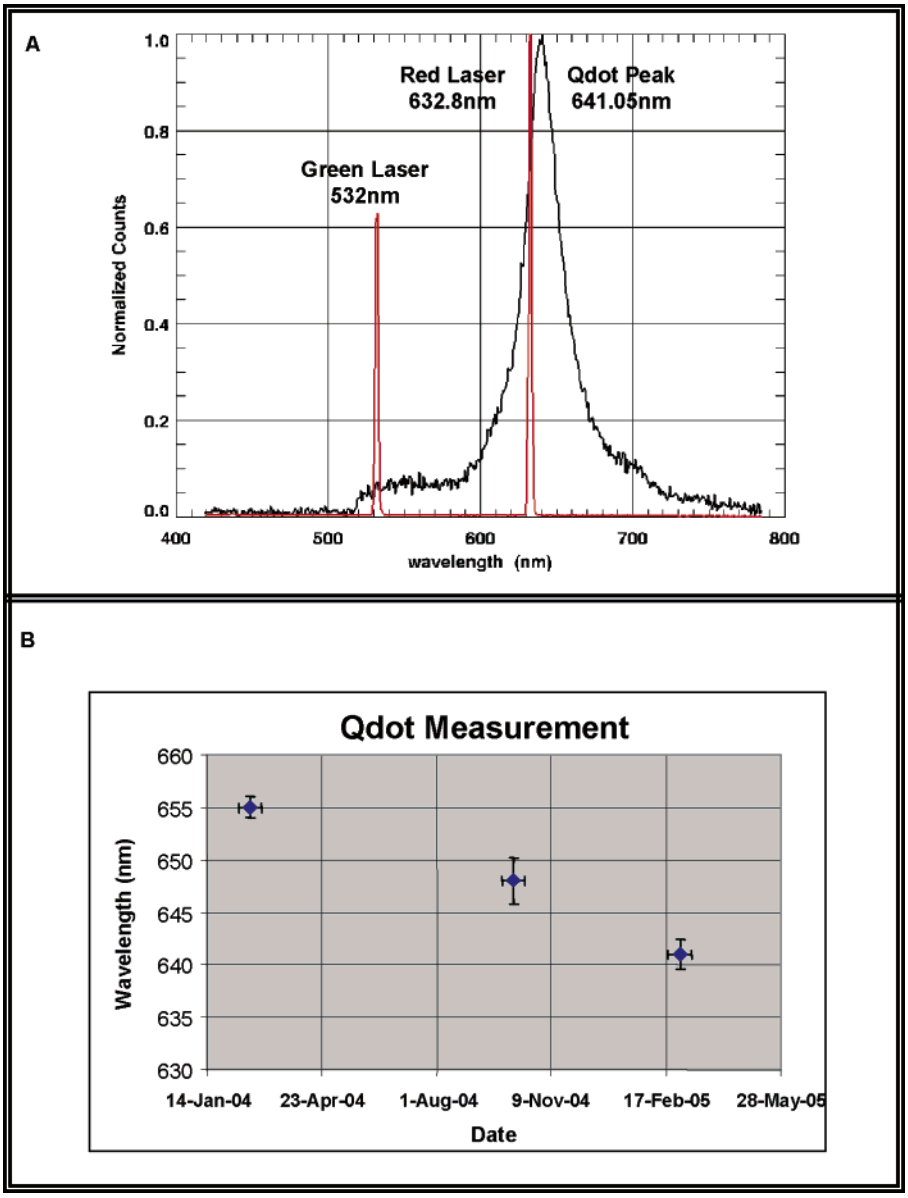

Figure 5. Overlay of laser calibration with the pixel to pixel Qdot signal measurement with the hyperspectral imaging microscope. Green (532 nm) and red (632.8 nm) lasers were used to calibrate the hyperspectral imaging microscope. The figure displays a pixel by pixel overlay of the QD and laser spectra (A). Multiple peaks were measured from different areas of the image acquisition cube. From the figure, the peak intensity of the QD is at 641 nm, which indicates a slight blue-shift of the 655 nm reported by the manufacturer when taking into account a combined error of ~1.414 nm. A plot of the measurements of the maximum wavelength vs time of measurement indicates a time-dependent decrease in the wavelength, possibly revealing erosion of the outer QD shell (B).

parallel. Because this imaging technique measures spectral signatures over a given bandwidth and does not simply count photons passed through a narrow-bandwidth filter, overlapping fluorescent spectra can be read in parallel on a single protein spot in our assay format. One can now envision the multiplexed analysis of the same area of a microarray probed with various QD-conjugated biomolecules, each with a distinct emission peak. Thus, the amount of information that can be gleaned from a single RPMA is dramatically enhanced. Integration of QD technology into protein microarray platforms will likely provide a means for subtle measurements of intracellular signaling pathways while surveying multiple molecular targets simultaneously through multiplexing at subcellular localization resolution.

QDs have remarkably high photochemical stability and can withstand numerous illumination cycles compared to organic fluorophores that get bleached much more rapidly, as exemplified by the extended analytical shelf life of our protein arrays. Extended integration times are thus possible, as are improved signal-to-noise ratios, enhanced sensitivity, enhanced quantitation, and increased assay reliability. For clinical samples in which the concentrations of target proteins may vary considerably, one array may need to be exposed multiple times in order to image widely varying concentrations of analytes. The QDs promote tailored imaging at multiple time intervals for each array on the basis of the signal level present within each sample. Chromogenic arrays do not permit this flexibility, and organic fluorophores rapidly degrade upon repeated imaging. Of note in this study, the QD signal showed remarkable longevity, with unamplified signal present over six months after the initial testing using a hyperspectral imager analyzer. This quality is a very attractive attribute as the protein microarray moves toward clinical usage; however, there may be a time-dependent change in wavelength associated with this signal.

A change in QD wavelength has been reported before, and a mechanism has been suggested. Ballou et al. (2004) pointed out that QD coatings do break down and do remain fluorescent for at least four months (*25*). If the PEG shell of the Qdot 655-PEG-Sav reagent erodes and the ZnS shell is breached or eroded, the Cd and Se atoms could wear down in addition. One report described ZnS shell erosion of QDs with a resultant blue-shift of the emission wavelength (*26*). However, this change was not described for the 655 nm quantum dot, and the shift shown is not large enough to account for the 14 nm we see in our last microarray scan by hyperspectral imaging. On the basis of published data (*26*), the wavelength changes ~43 nm for each 1 nm diameter change of CdSe. Our 14 nm change corresponds to a reduction in diameter of 3.2 Å; such a depth of erosion could be due to the removal of just 3 Cd and/or Se atoms from the surface of the core.

In conclusion, the potential for multiplexed assays, detection of unamplified signals, expanded dynamic range, and robustness under repeated and varying exposure periods makes QD nanoparticles especially suitable for clinical proteomics applications. The hyperspectral image analyzer enables a broadened use of QDs in RPMAs because of its sensitivity and multiplexing characteristics. Technological advances such as integration of QDs and hyperspectral imaging into RPMAs for molecular network analysis will hasten the advance of personalized assessments of patient tumor cells.

ACKNOWLEDGMENT

The authors wish to thank Theresa Harper (Quantum Dot Corporation) for her input into this study. Also, they wish to thank Mary Winters for providing Jurkat cell lysates. Animesh Nandi and Johanne Pastor provided insightful critiques of the manuscript. This work was supported by the University of Texas Southwestern Center for Proteomics Research contract from the NHLBI and the Hudson Foundation.

LITERATURE CITED

(1) Liotta, L. A., and Kohn, E. C. (2001) The microenvironment of the tumour-host interface. *Nature 411*, 375.
(2) Hunter, T. (2000) Signaling—2000 and beyond. *Cell 100*, 113.
(3) Liotta, L. A., Espina, V., Mehta, A. I., Calvert, V., Rosenblatt, K., Geho, D., Munson, P. J., Young, L., Wulfkuhle, J., and Petricoin, E. F., 3rd. (2003) Protein microarrays: meeting analytical challenges for clinical applications. *Cancer Cell 3*, 317.
(4) Grubb, R. L., Calvert, V. S., Wulkuhle, J. D., Paweletz, C. P., Linehan, W. M., Phillips, J. L., Chuaqui, R., Valasco, A., Gillespie, J., Emmert-Buck, M., Liotta, L. A., and Petricoin, E. F. (2003) Signal pathway profiling of prostate cancer using reverse phase protein arrays. *Proteomics 3*, 2142.
(5) Wulfkuhle, J. D., Aquino, J. A., Calvert, V. S., Fishman, D. A., Coukos, G., Liotta, L. A., and Petricoin, E. F., 3rd. (2003) Signal pathway profiling of ovarian cancer from human tissue specimens using reverse-phase protein microarrays. *Proteomics 3*, 2085.
(6) Paweletz, C. P., Charboneau, L., Bichsel, V. E., Simone, N. L., Chen, T., Gillespie, J. W., Emmert-Buck, M. R., Roth, M. J., Petricoin, I. E., and Liotta., L. A. (2001) Reverse phase protein microarrays which capture disease progression show activation of pro-survival pathways at the cancer invasion front. *Oncogene 20*, 1981.
(7) Morozov, V. N., Gavryushkin, A. V., and Deev, A. A. (2002) Direct detection of isotopically labeled metabolites bound to a protein microarray using a charge-coupled device. *J. Biochem. Biophys. Methods 51*, 57.
(8) Wiese, R. (2003) Analysis of several fluorescent detector molecules for protein microarray use. *Luminescence 18*, 25.
(9) Kukar, T., Eckenrode, S., Gu, Y., Lian, W., Megginson, M., She, J. X., and Wu, D. (2002) Protein microarrays to detect protein−protein interactions using red and green fluorescent proteins. *Anal. Biochem. 306*, 50.
(10) Alivisatos, P. (1996) Perspectives on the physical chemistry of semiconductor nanocrystals. *J. Phys. Chem. 100*, 13226.
(11) Alivisatos, P. (2004) The use of nanocrystals in biological detection. *Nat. Biotechnol. 22*, 47.
(12) Bruchez, M., Moronne, M., Gin, P., Weiss, S., and Alivisatos, A. (1998) Semiconductor nanocrystals as fluorescent biological labels. *Science 281*, 2013.
(13) Huebschman, M. L., Schultz, R. A., and Garner, H. R. (2002) Characteristics and capabilities of the hyperspectral imaging microscope. *IEEE Eng. Med. Biol. Mag. 21,* 104.
(14) Schultz, R. A., Nielsen, T., Zavaleta, J. R., Ruch, R., Wyatt, R., and Garner, H. R. (2001) Hyperspectral imaging: a novel approach for microscopic analysis. *Cytometry 43*, 239.
(15) Petricoin, E. F., Zoon, K. C., Kohn, E. C., Barrett, J. C., and Liotta, L. A. (2002) Clinical proteomics: translating benchside promise into bedside reality. *Nat. Rev. Drug Discovery 1*, 683.
(16) Espina, V., Mehta, A. I., Winters, M. E., Calvert, V., Wulfkuhle, J., Petricoin, E. F., 3rd, and Liotta, L. A. (2003) Protein microarrays: molecular profiling technologies for clinical specimens. *Proteomics 3*, 2091.
(17) Boise, L. H., and Thompson, C. B. (1997) Bcl-x(L) can inhibit apoptosis in cells that have undergone Fas-induced protease activation. *Proc. Natl. Acad. Sci. U.S.A. 94*, 3759.
(18) Bobrow, M. N., Harris, T. D., Shaughnessy, K. J., and Litt, G. J. (1989) Catalyzed reporter deposition, a novel method of signal amplification application to immunoassays. *J. Immunol. Methods 125*, 279.
(19) Marshall, C. J. (1995) Specificity of receptor tyrosine kinase signaling: transient versus sustained extracellular signal-regulated kinase activation. *Cell 80*, 179.
(20) Chan, W., Maxwell, D., Gao, X., Bailey, R., Han, M., and Nie, S. (2002) Luminescent quantum dots for multiplexed biological detection and imaging. *Curr. Opin. Biotechnol. 13*, 40.
(21) Han, M., Gao, X., Su, J. Z., and Nie., S. (2001) Quantum-dot-tagged microbeads for multiplexed optical coding of biomolecules. *Nat. Biotechnol. 19*, 631.
(22) Watson, A., Wu, X., and Bruchez, M. (2003) Lighting up cells with quantum dots. *Biotechniques 34*, 296.
(23) Xu, Y., and Bao, G. (2003) A filtration-based protein microarray technique. *Anal. Chem. 75,* 5345.
(24) Akerman, M., Chan, W., Laakkonen, P., Bhatia, S., and Ruoslahti, E. (2002) Nanocrystal targeting in vivo. *Proc. Natl. Acad. Sci. U.S.A. 99*, 12617.
(25) Ballou, B., Lagerholm, B., Ernst, L., Bruchez, M., and Waggoner, A. (2004) Noninvasive imaging of quantum dots in mice. *Bioconjugate Chem. 15*, 79.
(26) Dabbousi, B. O., Rodriguez-Viejo, J., Mikulec, F. V., Heine, J. R., Mattoussi, H., Ober, R., Jensen, K. F., and Bawendi, M. G. (1997) (CdSe)ZnS core−shell quantum dots: synthesis and characterization of a size series of highly luminescent nanocrystrallites. *J. Phys. Chem. B 101*, 9463.

BC0497113